

# Spherical Crystallography: Virus Buckling and Grain Boundary Scars

DAVID R. NELSON

*Lyman Laboratory of Physics, Harvard University, Cambridge, MA 02138*

**Summary.** — Ordered states on spheres require a minimum number of topological defects. For the case of crystalline order, triangular lattices must be interrupted by an array of at least 12 five-fold disclination defects, typically sitting at the vertices of an icosahedron. For  $R \gg a$ , where  $R$  is the sphere radius and  $a$  the particle spacing, the energy associated with these defects is very large. This energy can be lowered, however, either by buckling, as appears to be the case for large viruses, or by introducing unusual finite length grain boundary scars. The latter have been observed recently for colloidal particles adsorbed onto water droplets in oil.

## 1. – Introduction

Understanding ordered states on curved surfaces like the sphere requires dealing with “geometrical frustration.” Order parameters which describe crystalline or hexatic order in the centers of mass of the microscopic degrees of freedom, or the projections of tilted molecules onto a local tangent plane, often minimize their energy by aligning in neighboring regions. It is natural to assume that this alignment can be achieved by parallel transport of the vector or tensor order parameter which represents the local order [1, 2]. In a continuum description, the required parallel transport can be described by connection coefficients which couple to the displacement or phase angle much like a vector potential couples to the phase of a Type II superconductor [3]. However, such alignment cannot be achieved everywhere when a nonzero Gaussian curvature is present. In particular, an attempt to produce a vector field aligned by parallel transport fails on a loop which contains a net integrated Gaussian curvature [4]. The Gaussian curvature embodied in the line integral of the connection coefficients around the loop resembles the frustration in a superconducting order parameter produced by a nonzero magnetic field [5].

Consider  $N$  particles with a repulsive hard core interaction closed-packed on the surface of a sphere. If  $R$  is the radius of sphere,  $N \sim (R/a)^2$ , where  $a$  is the hard core diameter. Now imagine “triangulating” this sphere by connecting nearest neighbor particles using the spherical analogue of the familiar Wigner-Seitz construction of solid

state physics. The geometric frustration discussed above appears on a more microscopic level in Euler’s theorem [6] on a sphere, which states the number of triangles  $T$ , edges  $E$  and vertices  $N$  of such a tessellation are related,

$$(1) \quad T - E + N = 2.$$

Each edge is shared with two triangles, but a single triangle has three edges, so  $T = \frac{1}{3}(2E)$  and Eq. (1) can be rewritten as  $N - \frac{1}{3}E = 2$ . If the coordination numbers at each node in this triangulation are denoted  $Z_j$ , then  $E = \frac{1}{2} \sum_j Z_j$  and Euler’s theorem constrains the deviations of the  $\{Z_j\}$  from 6 on any surface with the topology of a sphere,

$$(2) \quad \sum_{j=1}^N (6 - Z_j) = 12.$$

Although identical particles with a hard core repulsion in a plane typically pack into a triangular lattice with six-fold coordination, on a sphere Eq. (2) shows that there must be at least 12 five-fold disclinations as well as an arbitrary number of six-coordinated sites. The 12 extra disclination defects (each representing a rotational discontinuity of  $2\pi/6$ ) can be viewed as a consequence of the geometrical frustration associated with the Gaussian curvature of a sphere, which integrates to  $4\pi = 12 \times (2\pi/6)$ . One plausible candidate for the ground state of an array of particles on the sphere is a “superlattice” of these disclinations (rather like the Abrikosov flux lattice of a Type II superconductor) arrayed at the vertices of a regular icosahedron.

Although this hypothesis is likely to be approximately correct for the ground state of  $N$  interacting particles on a sphere for moderate values of  $R/a$ , the very large energy associated with the twelve isolated disclinations makes this guess questionable when  $R/a$  becomes large. In fact, the extra energy due to the disclinations (relative to a perfect triangular lattice in flat space) grows like  $YR^2$  (see Sec. 2), where  $Y$  is a two-dimensional Young’s modulus. In this review, we briefly sketch two ways of reducing this energy. The first, relevant to hollow spherical shells which can be used to model viruses, invokes a buckling transition of the 12 disclinations and leads to a *faceted* icosahedral shape [7]. If  $\kappa$  is bending rigidity of the spherical shell, the  $YR^2$  behavior of the disclination energies is replaced by  $\kappa \ln(R/a)$  for large  $R$ . Another mechanism takes over for particles packed on a large spherical droplet, where surface tension limits significant buckling of disclinations out the local tangent plane. Even in this case, the energy can still be reduced by introducing grain boundaries which radiate from the 12 disclinations [8]. The energy now grows like  $E_c(R/a)$ , where  $E_c$  is a dislocation core energy. This energy is larger than if buckling of the disclinations were allowed, but still smaller than the amount  $\sim YR^2$  characteristic of isolated disclinations when  $R$  is large.

In Sec. 2, we review virus buckling, while Sec. 3 presents a brief discussion of grain boundary “scars” which have now been observed experimentally [9].

## 2. – Theory of Virus Shapes

Understanding virus structures is a rich and challenging problem [10], with a wealth of new information now becoming available. Although traditional X-ray crystallography

still allows the most detailed analysis [11], three-dimensional reconstructions of icosahedral viruses from cryo-electron micrographs are now becoming routine [12]. Electron microscope images of many identical viruses in a variety of orientations are used to reconstruct a three-dimensional image on a computer, similar to CT (computed tomography) scans in medical imaging. There are now, in addition, beautiful single molecule experiments which measure the work needed to load a virus (bacteriophage  $\phi 29$ ) with its DNA package [13]. It is of some interest to explore the elastic parameters and physical ideas which determine the shapes of viruses with an icosahedral symmetry.

The analysis of approximately spherical viruses dates back to pioneering work by Crick and Watson in 1956 [14], who argued that the small size of the viral genome requires identical structural units packed together with an icosahedral symmetry. These principles were put on a firm basis by Don Caspar and Aaron Klug in 1962 [15], who showed how the proteins in a viral shell (the “capsid”) could be viewed as icosadeltahedral triangulations of the sphere by a set of pentavalent and hexavalent morphological units (“capsomers”). The viral shells (there can also be an outer envelope composed of membrane elements from the host cell) are characterized by a pair of integers  $(P, Q)$  such that the number of morphological units is  $N = 10(P^2 + PQ + Q^2) + 2$ . To get from one pentavalent capsomer to another, one moves  $P$  capsomers along a row of near-neighbor bonds on the sphere, turns 60 degrees and moves another  $Q$  steps. The Euler theorem discussed in the Introduction insures that the number of capsomers in five-fold environments is exactly 12. A simple icosahedron of 12 morphological units corresponds to  $(1,0)$  while soccer balls and  $C_{60}$  fullerene molecules are  $(1,1)$  structures with 32 polygons. An icosadeltahedron with symmetry indices  $(3,1)$  is shown in Fig. 1. The polyoma virus (SV40) is a  $(2,1)$  structure with 72 capsomeres, while the much larger adenovirus and herpes simplex virus are  $(5,0)$  and  $(4,0)$  structures with 252 and 162 morphological units, respectively. Structures like that in Fig. 1 with  $P$  and  $Q$  nonzero and  $P \neq Q$  are chiral.



Fig. 1. – A right-handed  $(3,1)$  triangulated net (icosadeltahedron) used to describe virus structure. The  $(1,3)$  structure is left-handed.

Note that the relatively small polyoma virus (diameter 440 Angstroms) is round (see Fig. 2a), while the much larger herpes simplex virus (diameter 1450 Angstroms) has a more angular or faceted shape [16] (see Fig. 2b). Faceting of large viruses is in fact a

common phenomenon; the protein subunits of different viruses, moreover, have approximately the same molecular weight [17]. If these protein assemblies are characterized by elastic constants and a bending rigidity [18], it is interesting to ask how deviations from a spherical shape develop with increasing virus size.

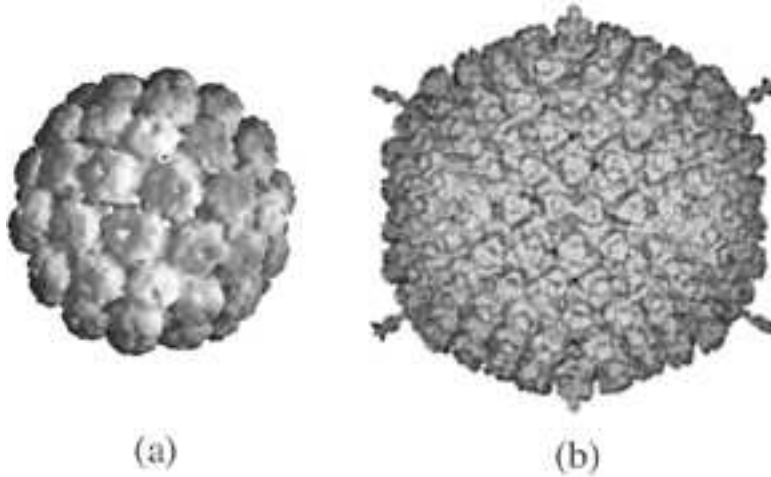


Fig. 2. – The polyoma virus (a) is approximately spherical while the larger adenovirus (b) is more faceted (not to scale) [16].

The faceting of large viruses may in fact be caused by a buckling transition associated with the 12 isolated points of 5-fold symmetry. These singularities can be viewed as disclinations in an otherwise 6-coordinated medium. It is well known that the large strains associated with an isolated disclination in a *flat* disk of triangular lattice leads to buckling into a conical shape for [1, 19]

$$(3) \quad YR^2/\kappa \geq 154,$$

where  $Y$  is the two-dimensional Young's modulus,  $\kappa$  is the bending rigidity and  $R$  is the disk radius. The energy of a single 5-fold disclination with “charge”  $s = 2\pi/6$  centered in a flat array of proteins of size  $R$  is approximately

$$(4) \quad E_5 \approx \frac{1}{32\pi} s^2 Y R^2.$$

However, above a critical buckling radius  $R_b \approx \sqrt{154\kappa/Y}$ , is there a conical deformation with [19]

$$(5) \quad E_5 \approx (\pi/3)\kappa \ln(R/R_b) + \frac{1}{32\pi} s^2 Y R_b^2.$$

One might expect a similar phenomenon for 12 disclinations confined to a surface with a spherical topology. Indeed, the elastic energy for 12 disclinations on an undeformed sphere of radius  $R$  is has a form similar to Eq. (4), namely [8]

$$(6) \quad E \approx 0.604(\pi Y R^2/36),$$

where the sphere radius  $R$  now plays the role of the system size. Although it seems highly likely that these 12 disclinations can lower their energy by buckling for large  $R$ , the nonlinear nature of the underlying elastic theory [18] leads to complex interactions between the resulting conical deformations. A boundary layer analysis of the von Karman equations for bent plates predicts anomalous scaling for the mean curvature in the vicinity of the ridges connecting conical singularities [20]. Interesting scaling behavior also arises in the vicinity of the apexes of the cones themselves [21]. Another intriguing physical realization of the buckling problem (with  $R/a \gg 1$  so that boundary layers near ridges are important) lies in the faceting of lecithin vesicles at temperatures sufficiently low so that the lipid constituents have crystallized [22].

To search for a buckling transition in viral capsids or crystalline vesicles, one must study the strains and ground states of crystalline particle arrays with 12 disclinations in a spherical geometry [7]. The nonlinear Foppl-von Karman equations for thin shells with elasticity and a bending energy can be treated using a floating mesh discretization developed and studied extensively in the context of “tethered surface” models of polymerized membranes [23]. By taking the nodes of the mesh to coincide with the capsomers, even small viruses can be handled in this way, although any buckling transition will surely be smeared out unless  $R_b/a$  is large, where  $a$  is the spacing between morphological units. Ideas from continuum elastic theory will, of course, be most applicable for vesicles composed of many lipids and for large viruses — Viruses with as many as 1692 morphological units have been reported [24].

There may be inherent limitations on the size of viral capsids that follow from the elastic properties of thin shells. Because larger viruses can accommodate more genetic material, larger sizes could confer an evolutionary advantage. If, however, large viruses buckle away from a spherical shape, the resistance of the capsid to mechanical deformation will degrade. A theory of buckled crystalline order on spheres allows estimates of important elastic parameters of the capsid shell from structural data on the shape anisotropy [7]. Although some aspects of virus structure could be accounted for by the physics of shell theory, other features could be more relevant to cell recognition, avoidance of immune response, etc. Estimates of quantities such as the bending rigidity and Young’s modulus of an empty viral shell might allow an understanding of deformations due to loading with DNA or RNA [13].

The results of recent investigations of buckling transitions in a spherical geometry using the methods of Refs. [19] and [23] are illustrated in Fig. 3 [7]. Spherical shells do indeed become aspherical as the “von Karman number”  $YR^2/\kappa$  increases from values of order unity to  $YR^2/\kappa \gg 1$ . The mean square “asphericity” (deviation from a perfect spherical shape) departs significantly from zero when  $YR^2/\kappa$  exceeds 154, the location of the buckling transition in flat space. Note that fits of buckled viruses or crystalline vesicles to this universal curve would allow an experimental estimate of the ratio  $Y/\kappa$ . More quantitative information on the buckled shape can be extracted by expanding the radius  $R(\theta, \phi)$  in spherical harmonics,

$$(7) \quad R(\theta, \phi) = \sum_{\ell=0}^{\infty} \sum_{m=-\ell}^{\ell} Q_{\ell m} Y_{\ell m}(\theta, \phi),$$

and studying the rotationally invariant quadratic invariants allowed for icosahedral viruses

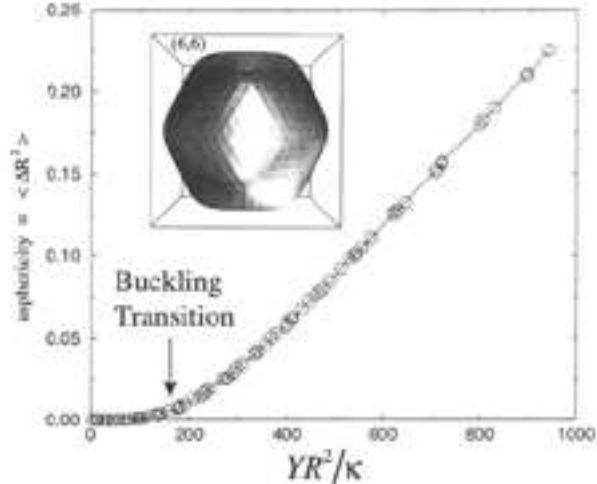


Fig. 3. – Mean square asphericity as a function of  $YR^2/\kappa$  for many different icosadeltahedra. The inset shows a (6,6) structure with  $YR^2/\kappa \approx 1000$ .

or vesicles, namely

$$(8) \quad \hat{Q}_\ell = \sqrt{\frac{1}{2\ell+1} \sum_{m=-\ell}^{\ell} |Q_{\ell m}|^2 / Q_{00}}$$

with  $\ell = 0, 6, 10, 12, 16, 18, \dots$  [25]. Although *any* parameter set of the form  $\{\hat{Q}_6, \hat{Q}_{10}, \hat{Q}_{12}, \dots\}$  could be consistent with an icosahedral symmetry, all buckled objects describable by the theory of elastic shells should in fact lie on a universal curve parametrized by the value of  $YR^2/\kappa$ . Deviations from this curve are presumably be of some biological interest. In addition to exploring shape changes induced by an internal pressure (A virus loaded with  $6 \mu\text{m}$  of DNA can have an internal pressure as large as 6 MPa! [13]), it would interesting to study the spontaneous membrane curvature produced by an asymmetric conical shape of the constituent proteins [26]. See Ref. [7] for more details and quantitative fits to the shapes of the HK97 virus and a yeast virus.

### 3. – Grain Boundary Scars

When particles are packed on a surface where the restoring force is a surface tension, instead of a bending rigidity, buckling is suppressed. For example, water droplets in oil coated with colloidal particles remain spherical even in the presence of disclinations in the colloidal array. Remarkably, the classical ground state of interacting particles confined to a frozen surface like a sphere is still a matter of debate [27], especially in the limit of large sphere radius  $R$  compared to the particle spacing  $a$ . This problem was first posed for interacting electrons by J. J. Thomson in 1904 [28]. Physical realizations include multi-electron bubbles in superfluid helium [29], and “colloidosomes” [30], which are lipid bilayers or droplets coated with colloidal particles. Colloidosomes are potential delivery vehicles for drugs, flavors and fragrances. To study the ground states of such

systems, one can analyze an effective free energy describing the physics of disclination arrays constrained to lie on an arbitrary two-dimensional surface. For spherical surfaces, the ground state for moderate  $R/a$  can be approximated by a triangular lattice with twelve 5-fold disclinations at the vertices of an icosahedron. Building on work by Alar Toomre [31] and by Michael Moore and collaborators [32], it is possible to construct a detailed theory of interacting defects on a frozen, spherical topography [8]. Although the buckling found in viruses is not allowed, the ground state for large  $R/a$  includes unusual finite length grain boundaries. The methods of Ref. [8] allow the direct minimization of the energy of, say, 26,000 interacting particles to be replaced by the much easier problem of finding the ground state of 132 interacting disclination defects, [see Fig. 4] with interactions determined by continuum elastic theory on the sphere. Excellent results can be obtained using the Young's modulus and the dislocation core energy of particles in flat space as input parameters. Work by Bausch *et al.* [9] on colloidal particles absorbed onto water droplets in oil indicates a conventional ground state with just 12 disclination defects for small  $R/a$ , but with extra dislocations associated with grain boundaries for  $R/a \geq 5$ , corresponding to particle numbers  $N \gtrsim N_c \approx 360$ . Both this critical value of  $N$  and the number of excess dislocations in the grain boundary arms for  $N > N_c$  can be estimated using the theory of Ref. [8], with good agreement with experiment.

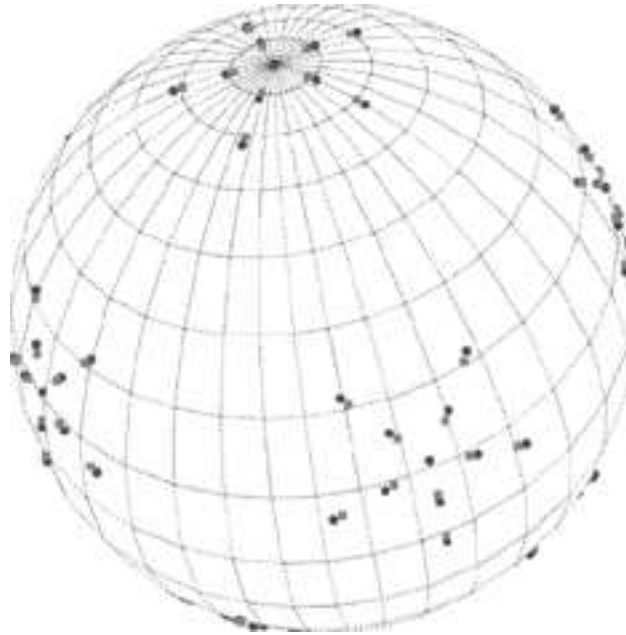


Fig. 4. – Dislocations emerging from 5-fold disclinations (circles) for a crystal of approximately 26,000 particles on a sphere [4]. Each dislocation is a 5–7 (circle-square) disclination *pair* in this representation.

See Ref. [33] for a discussion of the energetics of the crystalline state for large particle numbers and power-law potentials when *both* buckling and grain boundary scars are forbidden.

\* \* \*

The work described here was carried out in collaboration with M. Bowick, J. Lidmar, L. Mirny and A. Travasset. It is a pleasure to acknowledge these fruitful collaborations, as well as discussions with S. Harrison and A. Toomre. This work was supported by the National Science Foundation, through Grant DMR-0231631 and in part through the Harvard Materials Research Laboratory, via Grant DMR-0213805.

## REFERENCES

- [1] NELSON D.R. and PELITI L., *J. Physique*, **48** (1987) 1085.
- [2] DAVID F., in *Statistical Mechanics of Membranes and Surfaces*, edited by NELSON D.R., PIRAN T. and WEINBERG S. (World Scientific, Singapore) 1989.
- [3] TINKHAM T., *Introduction to Superconductivity*, 2nd ed. (McGraw-Hill, New York) 1996.
- [4] LANDAU L.D. and LIFSHITZ E.M., *The Classical Theory of Fields* (Pergamon, New York) 1971, Chapter 11.
- [5] See, e.g., NELSON D.R., *Phys. Rev. B*, **28** (1983) 5515.
- [6] COXETER H.S.M., *Introduction to Geometry* (Wiley, New York) 1969.
- [7] LIDMAR J., MIRNY L. and NELSON D.R., *cond-mat/030674*, *Phys. Rev. E*, (in press).
- [8] BOWICK M.J., NELSON D.R. and TRAVESSET A., *Phys. Rev. B*, **62** (2000) 8738 and references therein.
- [9] BAUSCH A.R., BOWICK M.J., CACCIUTO A., DINSMORE A.D., HSU M.F., NELSON D.R., NIKOLAIDES M.G., TRAVESSET A. and WEITZ D.A., *Science*, **299** (2003) 1716.
- [10] *Structural Biology of Viruses*, edited by CHIU W., BURNETT R.M. and GARCEA R.L., (Oxford University Press, New York) 1997.
- [11] HARRISON S.C., *Harvey Lectures*, **85** (1991) 127.
- [12] BAKER T.S., OLSON N.H. and FULLER S.D., *Microbiol. Molec. Biol. Rev.*, **63** (1999) 862.
- [13] SMITH D.E., TANS S.J., SMITH S.B., GRIMES S., ANDERSON D.L. and BUSTAMANTE C., *Nature*, **413** (2001) 748.
- [14] CRICK F. and WATSON J.D., *Nature*, **177** (1956) 473.
- [15] CASPAR D. and A. KLUG A., *Cold Spring Harbor Symp. on Quantitative Biology*, **27** (1962) 1.
- [16] REDDY V., NATARAJAN P., OKERBERG B., LI K., DAMODARAN K., BROOKS M.R. III and JOHNSON J., *Virus Particle Explorer (VIPER), a Website for Virus Capsid Structures and their Computational Analyses*, *J. Virology*, **75** (2001) 11943.
- [17] MURZIN A.G., BRENNER S.E., HUBBARD T. and C. CHOTHIA, *J. Mol. Biol.*, **247** (1995) 536.
- [18] LANDAU L.D. and LIFSHITZ I.M., *Theory of Elasticity* (Pergamon, New York) 1975.
- [19] SEUNG S. and NELSON D.R., *Phys. Rev. A*, **38** (1988) 1005.
- [20] LOBKOVSKY A.E. and WITTEN T.A., *Phys. Rev. E*, **55** (1997) 1577.
- [21] CERDA E. and MAHADEVAN L., *Phys. Rev. Lett.*, **80** (1998) 2358.
- [22] BLAUROCK A.E. and GAMBLE R.C., *J. Membrane Biol.*, **50** (1979) 187; see also DUBOIS M., DEMÉS B., GULIK-KRZYWICKI T., DEDIEU J.-C., VAUTRIN C., DESERT S., PERZ E. and ZEMB T., *Nature*, **411** (2001) 672.
- [23] KANTOR Y. and NELSON D.R., *Phys. Rev. A*, **36** (1987) 4020.
- [24] YAN X., OLSON N.H., VAN ETTEN J.L., BERGOIN M., ROSSMANN M.G. and BAKER T.S., *Nature Struct. Biol.*, **7** (2000) 101.
- [25] STEINHARDT P., NELSON D.R. and RONCHETTI M., *Phys. Rev. Lett.*, **47** (1981) 1297.
- [26] For an analogous exploration of the shapes of *liquid* membranes with a spherical topology, see SEIFERT U., *Advances in Physics*, **46** (1997) 13; for a discussion of viral shells, see BRUINSMA R.F., GELBERT W.M., REGUERA D., RUDNICK J. and ZANDI R., *Phys. Rev. Lett.*, **90** (2003) 248101.



- [27] SAFF E.B. and KUIJLAARS A.B.J., *The Math. Intellig.*, **19** (1997) 5.
- [28] THOMSON J.J., *Philos. Mag.*, **7** (1904) 237.
- [29] LEIDERER P., *Z. Phys. B*, **98** (1995) 303.
- [30] RAMOS L., LUBENSKY T.C., DAN N., NELSON P. and WEITZ D.A., *Surfactant-Mediated Two-Dimensional Crystallization of Colloidal Crystals*, *Science*, **286** (1999) 2325.
- [31] TOOMRE ALAR, unpublished work.
- [32] DODGSON M.J.W. and MOORE M.A., *Phys. Rev. B*, **55** (1997) 3816; PEREZ-GARRIDO A. and MOORE M.A., *Phys. Rev. B*, **60** (1999) 15,628.
- [33] BOWICK M., CACCIUTO A., NELSON D.R. and TRAVESSET A., *Phys. Rev. Lett.*, **89** (2002) 185,502.